IOP Conf. Series: Materials Science and Engineering **377** (2018) 012206 doi:10.1088/1757-899X/377/1/012206

Bond graph modelling and simulation of a variable inertia flywheel

S Samaddar[1*], P Kushwaha[2] , S K Ghoshal[1]
[1]Department of Mechanical Engineering, Indian Institute of Technology (ISM), Dhanbad Jharkhand -826004, India.
[2]Department of Mining Machinery Engineering, Indian Institute of Technology (ISM), Dhanbad Jharkhand -826004, India.
*Corresponding author's email address- ssprimex@gmail.com

Abstract. In this paper, a two terminal hydraulic cylinder-motor system attached to a variable inertia flywheel is modelled and simulated to investigate its dynamic performance. In contrast to the constant inertial flywheel, the variable inertia flywheel takes care of the jerk of the dynamic system at the time of fast speed change or sudden speed reversal by suitably adapting its moment of inertia. Bond graph simulation technique is used to model the system as it is a unified strategy suitable for multi-domain modelling

1. Introduction

Springs and flywheels are mostly considered as energy storing devices particularly in mechanical systems. Springs can absorb and release very small amount of energy for a short period of time, as its design is based on the resilience criterion of the material [1]. Therefore, there is limitation in energy storage for the springs. On the other hand, flywheel is an important mechanical device for storing kinetic energy over a complete cycle. A flywheel is specifically designed to efficiently store rotational energy. Flywheels resist changes in rotational speed by their moment of inertia [2]. The moment of inertia for a flywheel is given by the product of the mass and square of the distance of the mass point from the axis of rotation. Earlier constant and stable energy supply for flywheels, posed a great problem, as the moment of inertia has to be adjusted [3], for different rotational velocities in different situations and thus energy supply would fluctuate a lot.

With the concept and introduction of variable inertia flywheels, the idea for energy storage has completely changed. No matter whatever be the rotational speed of the flywheel, whether low, medium, or high, the flywheel can supply a stable and constant energy to the system when required, as the variable inertia of the flywheel automatically changes the inertia of the system with the input and response as the application requires. The approach and simplicity of the design in the variable inertia flywheel, has made energy storage very attractive [4]. The applications of the variable inertia flywheel are tremendous. It has a very high potential for passive vibration control [5] and can be used in regenerative braking [6].

Previous work has not revealed anything about the dynamic behaviour of the system, rather identification and validation of the system parameters has been the main objective. The results obtained satisfies the mathematical and experimental work.

2. The Variable Inertia Flywheel

A schematic diagram and prototype of the variable inertia flywheel is shown in figure 1. The overall dimension of the flywheel is given in table 1. It is basically a flywheel frame having a circular plate in which four slots has been made. Slider masses and a springs is placed inside the slots. The movement of the sliders within the slots and compressing of the springs is provided by the rotational motion of the flywheel. As the speed of rotation varies, it leads to the changes in the slider location within the slots which changes the moment of inertia of the flywheel and ultimately changes the equivalent inertial mass of the flywheel.

Figure 1 The variable inertia flywheel (a) schematic diagram and (b) prototype (1-spring, 2-inner hole for the shaft, 3-slot, 4-slider and 5-frame)

The moment of the inertia of the solid circular disk including the slots (I_{fz}) is given by

$$I_{fz} = \frac{1}{2} m_f (r^2 + R^2) \quad (1)$$

where, the terms m_f, r and R denotes the mass of the flywheel including the slots, radius of inner hole and outer radius of the flywheel respectively. The moment of inertia of one slot (I_{oz}) is expressed as

$$I_{oz} = \frac{1}{12} m_o (d^2 + a^2) + m_o (R - \frac{1}{2} a) , \quad (2)$$

where, the term ($R - {}^{1}/_{2}\, a$) indicates the distance between the rotation centre of the flywheel and the centroid of a slot. The terms a and d indicates the length and width of the slot respectively and m_o indicates the mass of the removed slot material. The moment of inertia of one slider (I_{sz}) is given by

$$I_{sz} = \frac{1}{12} m_s \left(\frac{3}{4} d^2 + l_s^2\right) + m_s l^2 \quad (3)$$

The terms m_s, l_s and d, hereby denotes the mass, length and width of the slider respectively. The term l indicates the location of the slider masses within the slots of the variable inertia flywheel which changes with the rotational speed. From the schematic diagram shown in figure 1, the moment of the variable inertia flywheel is expressed as (I_{af})

$$I_{af} = I_{fz} - 4I_{oz} + 4I_{sz} \quad (4)$$

The slider location and angular velocity is related by equating the centrifugal force acting on the sliders and spring forces of the variable inertia flywheel. Mathematically it can be represented as

$$m_s \omega^2 l = k_s (l - l_{min}) \quad (5)$$

Here the terms m_s, k_s, l_{min} and ω indicates the mass of the slider, stiffness of the spring, minimum length of the sliders within the slots of the flywheel and rotational speed of the variable inertia flywheel respectively.

Considering ideal situation of the two-terminal hydraulic device, the flow rate through the one chamber to another is expressed as

$$\dot{Q} = \omega h \quad (6)$$

where, ω and h represents the angular velocity of the variable inertia flywheel and displacement of the hydraulic motor respectively. As

$$\omega = v_a \frac{A}{h} \quad (7)$$

where v_a represents the linear relative input velocity from the two-terminals of the hydraulic device and A denotes the cross-sectional area of the cylinder, excluding the cross-sectional area of the rods of the piston from both sides. Equations (5), (6) and (7) gives the final mathematical form of the slider location within the slot of the variable inertia flywheel as

$$l = \frac{k_s l_{min}}{k_s - m_s \left(\frac{v_a A}{h}\right)^2} \quad (8)$$

The terms l_{min} and k_s represents the minimum distance of the slider masses within the slots of the flywheel and stiffness of the spring respectively. Equation (8) reveals that the maximum distance of the slider masses within the slots of the variable inertia flywheel can theoretically reach infinite value. This is physically impossible as there is a provision for restriction by outer flywheel ring. No matter with whatever high magnitude the flywheel rotates, it always stays within a safe limit provided by the outer

flywheel ring. The minimum and maximum distance of the slider mass in the slot of the variable inertia flywheel is calculated as 0.0025 m and 0.0375 m respectively.
From the data given in Table 1, the moment of the inertia of the variable inertia flywheel (I_{af}), is calculated as

$$I_{af} = (8.83 \times 10^{-4} + 0.14l^2) \quad (9)$$

The moment of inertia of the flywheel (I_{af}), leads to equivalent inertia mass of the variable inertia flywheel m_a which is expressed as

$$m_a = I_{af}\left(\frac{A}{h}\right)^2 \quad (10)$$

3. The physical system and its mathematical model

The variable inertia flywheel along with the two-terminal hydraulic device is shown in figure 2.

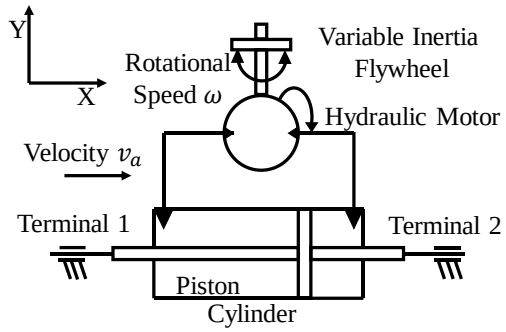

Figure 2. The two terminal hydraulic device with a variable inertia flywheel

The velocity input (v_a) through the two terminals causes the liquid to flow, which produces enough torque to rotate the hydraulic motor. This in turn rotates the flywheel coupled to the hydro-motor shaft. The dynamical performance of the system is analysed using Bond Graph Simulation. The Bond Graph model of the system is differentially causalled and then is converted into a diagnostic Bond Graph form. With the help this tool, parameter adjustment is done to achieve the results that earlier posed limitation on the dynamic behaviour of the variable inertia flywheel of the previous work. It eventually calculates the magnitude of the forces acting in the system for various input data. The net force acting in the entire system represented in figure 2, is given by

$$\left\{\begin{array}{l} F = m_a\dot{v}_a + b_a v_a + F_f \\ F_f = |F_f| sgn\,(v_a) \end{array}\right\} \quad (11)$$

The friction force in the system is taken into account as shown in equation (11). The friction force F_f always acts opposite to that of the linear relative input velocity v_a of the two-terminals of the hydraulic device. The terms b_a is the damping ratio of the system and $\dot{v}_a$ is the acceleration of the input response provided to the system. The Bond graph model of the entire setup for the variable inertia flywheel is presented in figure 3.

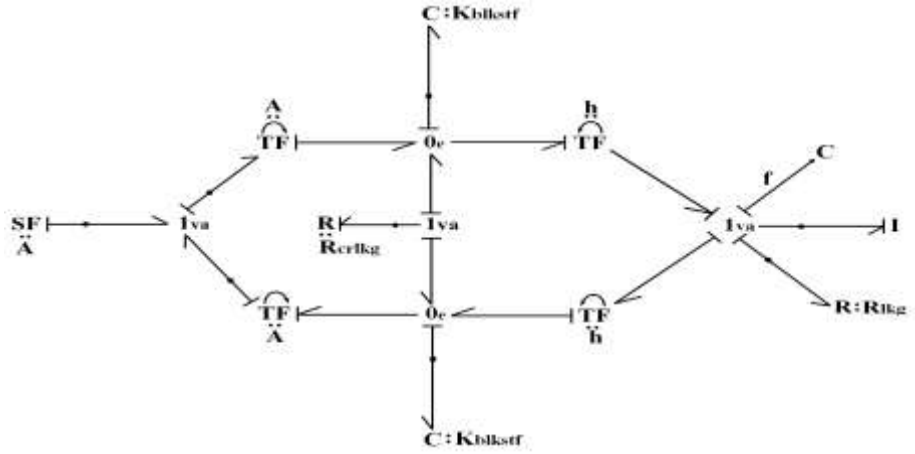

Figure 3 Bond Graph Model of the variable inertia flywheel with two-terminal hydraulic device

The notations for the bond graph model is presented in table 1. 1_{va} and 0_e represents flow summing and effort summing junctions respectively whereas f denotes the angular velocity acting in flywheel.

4. Results and discussions

To calculate the maximum and minimum moment of inertia of the variable inertia flywheel, a sinusoidal input of amplitude = 0.0314 m/s and frequency = 0.1 is provided. With this input the slider mass of the flywheel travels the maximum and minimum distance within the slots made in the flywheel without residing at a fixed place. Figure 4(b), (c) and (d) depicts that the behaviour the slider location, moment of inertia and equivalent mass of the flywheel respectively with sinusoidal input of amplitude = 0.0314 m/s and frequency = 0.1Hz. The maximum value and minimum magnitudes of the inertia for the variable inertia flywheel is calculated as $I_{af,max} = 1.08 \times 10^{-3}\ kgm^2$ and $I_{af,min} = 0.94 \times 10^{-3}\ kgm^2$ which agrees greatly with the theoretical calculation, provided by equation (8). Similarly, the maximum value and minimum equivalent inertia mass for the variable inertia flywheel is calculated as $m_{af,max} = 970.66\ kg$ and $m_{af,min} = 882.14\ kg$

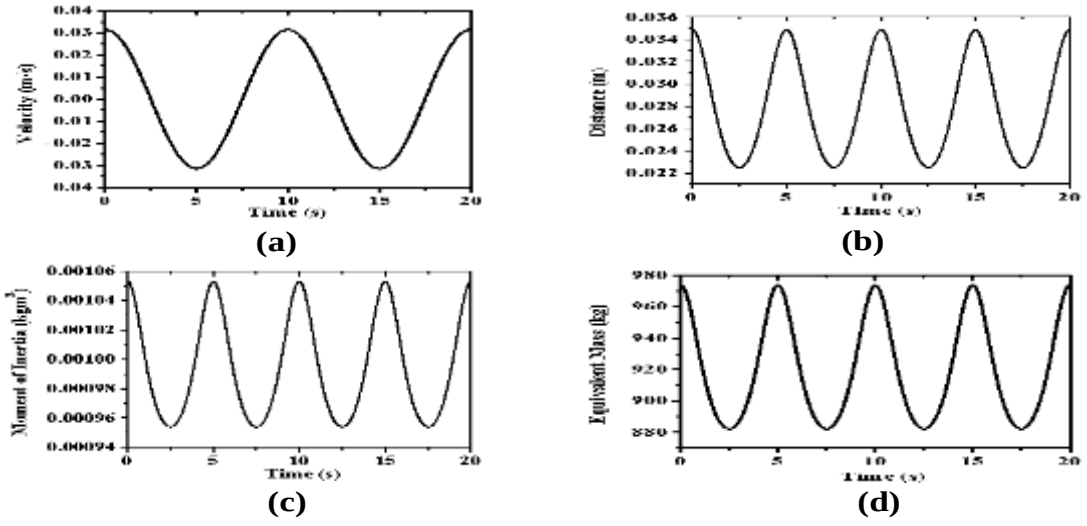

Figure 4. Time response of the variable inertia flywheel (a) input sinusoidal velocity (frequency = 0.1 Hz and amplitude = 0.0314 m/s), (b) slider location of the slider masses within the slots of the flywheel, (c) moment of inertia of the flywheel, (d) equivalent mass of the variable inertia flywheel

The behaviour and magnitude of the forces attained for the square inputs (a) frequency = 0.5 Hz and amplitude = 0.005 m/s and (b) frequency = 1 Hz and amplitude = 0.01 m/s respectively is shown in

figure 5. The peak value of the forces is determined as 653.41 N for figure 5(a) and 1309.65 N for figure 5(b) respectively.

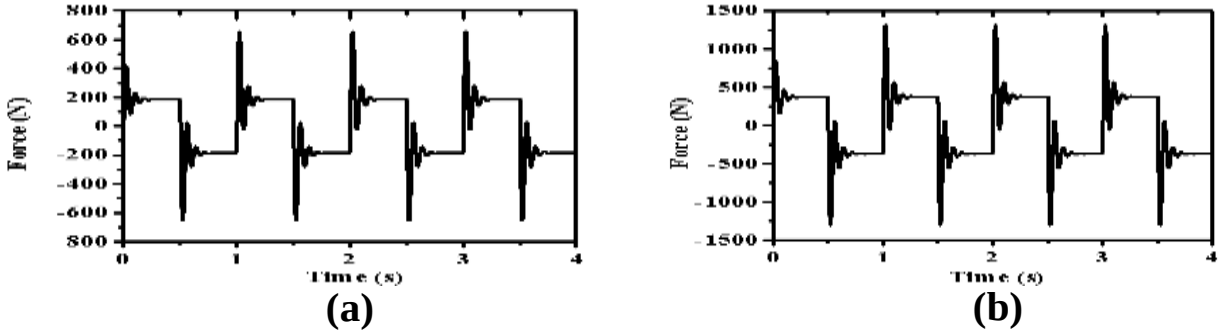

Figure 5. Time response of reactive force at the hydraulic cylinder terminal subject to square wave velocity input (a) frequency = 0.5 Hz and amplitude = 0.005 m/s, (b) frequency =1 Hz and amplitude = 0.01 m/s.

For the sinusoidal input provided into the system of frequency = 0.4 Hz and amplitude = 0.012 m/s and the other having frequency = 2 Hz and amplitude = 0.063 m/s respectively, the behaviour and magnitude of the forces attained is shown in figure 6. The peak value of forces is calculated as 445.09 N for figure 6(a) and 3516.44 N for figure 6(b) respectively.

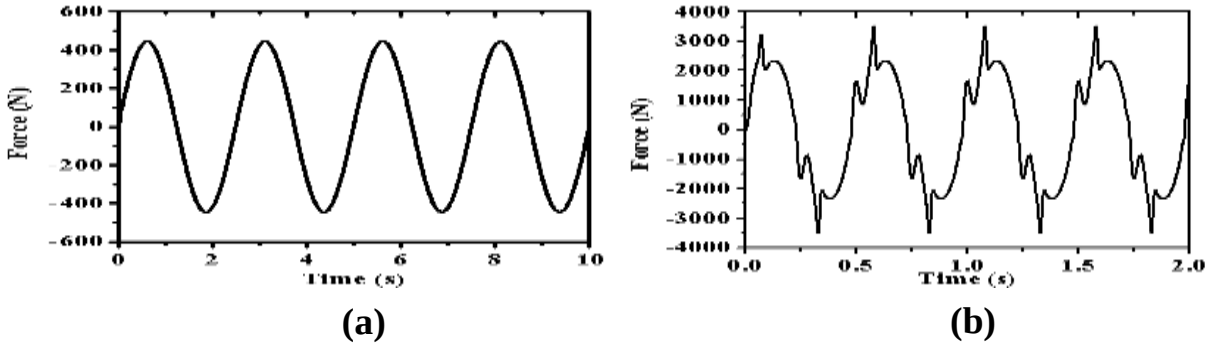

Figure 6. Time response of reactive force at the hydraulic cylinder terminal subject to sinusoidal wave velocity input (a) frequency = 0.4 Hz and amplitude = 0.012 m/s, (b) frequency = 2 Hz and amplitude = 0.063 m/s.

Other sets of sinusoidal inputs ranging from low to high frequencies is given to the system. The behaviour and magnitude of forces for different sinusoidal inputs of low frequency = 0.4 Hz and amplitude = 0.012 m/s, medium frequency = 1 Hz and amplitude = 0.0314 m/s and high frequency = 2 Hz and amplitude = 0.126 m/s is shown in figure 7 respectively. The peak value of the forces is given as 445.09 N for figure 7(a) 1200.76 N for figure 7(b) and 5296.15 N for figure 7(c) respectively.

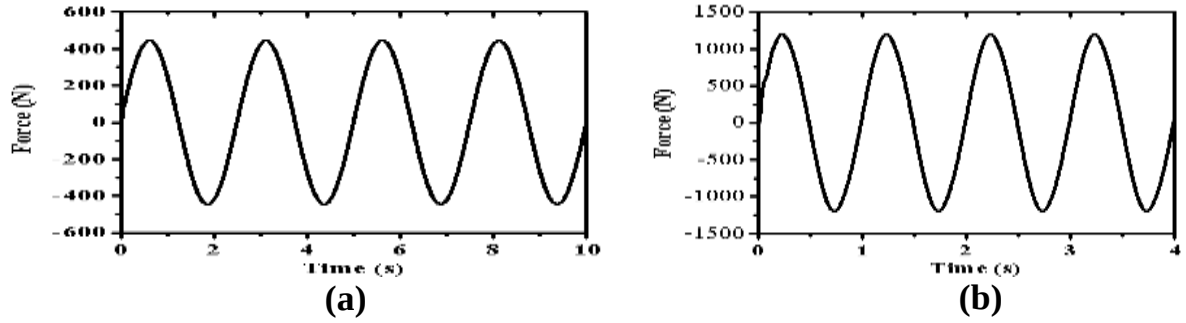

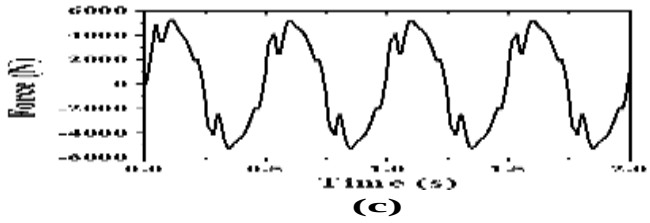

Figure 7. Time response of reactive force at the hydraulic cylinder terminal subject to sinusoidal wave velocity input (a) frequency = 0.4 Hz and amplitude = 0.012 m/s, (b) frequency = 1 Hz and amplitude = 0.0314 m/s and (c) frequency = 2 Hz and amplitude = 0.126 m/s.

Table 1 Parameters for the variable inertia flywheel with two-terminal hydraulic device

No	Name	Notations	Values
1	Radius of the inner hole	r	0.01 m
2	Outer radius of the flywheel	R	0.047 m
3	Length of the slot	a	0.03 m
4	Width of slot (diameter of slider)	d	0.02 m
5	Length of the slider	l_s	0.015 m
6	Stiffness of spring	k_s	90 N/m
7	Mass of slider	m_s	0.035 kg
8	Mass of flywheel (including slots)	m_f	1 kg
9	Mass of the removed slot material	m_o	0.079 kg
10	Cross-sectional area of the cylinder	A	$0.001256\, m^2$
11	Displacement of the hydraulic motor	h	$1.306 \times 10^{-6}\, m^3/rad$
12	Bulk stiffness of the fluid	K_{blkstf}	$2 \times 10^{12}\, N/m^2$
13	Cross flow leakage through port of hydraulic device	R_{crlkg}	$1 \times 10^{15}\ m^3/s$
14	Leakage loss through the cylinder	R_{lkg}	$4 \times 10^{-12}\ m^3/s$
15	Damping ratio	b_a	8100 N
16	Friction force	F_f	190 N

5. Conclusion

This paper illustrates about the dynamical nature of the variable inertia flywheel with two-terminal hydraulic device system. The results obtained from bond graph simulation concludes that the behaviour is in good agreement with the input responses provided to the system. Moreover, the output nature of the forces attained is almost similar with input responses. The results also justifies that for the variable inertia flywheel, the force generated within the system varies accordingly, leading to variable inertia force.

6. References

[1] Xu T, Liang M, Li C and Yang S 2015 Design and analysis of a shock absorber with variable moment of inertia for passive vehicle suspensions *J. Sound Vib.* **355** 66–85

[2] Metwalli S M, Shawki G S A and Sharobeam M H 2017 Optimum Design of Variable- Material Flywheels *J . Mechanisms, Transmissions, and Automation In Design* **105** 249–53

[3] Van de Ven J. 2009 Fluidic Variable Inertia Flywheel In *Proc. of 7th International Energy Conversation Engineering Conference* 1-6

[4] Ullman D and Velkoff H 1979 An Introduction to the Variable (vif) *J. Applied Mechanics* **46** 186–190

[5] Yang S and Baddour N 2016 Design , Modeling and Testing of a Two-Terminal Mass Device With a Variable Inertia Flywheel *J. Mechanical Design* **138** 1–10

[6] Figliotti M P 2014 A variable inertia flywheel model for regenerative braking on a bicycle *Proc. ASME 2014 Dyn. Syst. Control Conf.* 1–10